

Comparison of the Effective Radiation Dose in the Region of the Facial Skull Between Multidetector CT, Dental Conebeam CT and Intraoperative 3D C-Arms

Craniomaxillofacial Trauma &
Reconstruction
2024, Vol. 17(4) 270–278
© The Author(s) 2023



Article reuse guidelines:
sagepub.com/journals-permissions
DOI: 10.1177/19433875231213906
journals.sagepub.com/home/cmt



Sebastian Pietzka, MD, DMD^{1,2} , Anne Grieser, DMD², Karsten Winter, PhD³,
Alexander Schramm, MD, DMD^{1,2}, Marc Metzger, MD, DMD⁴,
Wiebke Semper-Hogg, MD, DMD⁴, Michael Grunert, MD⁵ , Marcel Ebeling, MD, DMD²,
Andreas Sakkas, MD, DMD^{1,2} and Frank Wilde, MD, DMD^{1,2}

Abstract

Study Design: Experimental single-centre study of X-ray absorption using a phantom skull.

Objective: This experimental study aimed to compare the radiation doses of different 3D imaging devices used in maxillofacial surgery, including one Multidetector CT (MDCT), two Conebeam CT (CBCT) and four intraoperative 3D C-arms.

Methods: Thermoluminescent dosimeters (TLD) were used to determine the absorbed radiation in an Alderson-Rando phantom skull. The phantom skull was positioned in the before mentioned seven devices and a defined 3D facial skull image was acquired. Subsequently, the TLD'S were read out and the effective doses (ED) and the organ doses (OD) were calculated and compared.

Results: OD varied significantly between tissues as well as between the 3D X-ray devices. The OD of the 3D C-arms were significantly lower than those of all other devices. The OD of the CT, especially in the standard setting, was the highest. Only by special adjustments of the scan protocol regarding CMF requirements for traumatology, the MDCT could achieve almost equivalent doses as the two tested CBCT-scanners. The calculated effective doses were also lowest for the 3D C-arm devices (11.2 to 129.9 μ Sv). The ED of the MDCT were significant higher (284.52–844.97 μ Sv) than in all other devices. The ED of the CBCTs (173.7–184.9) were lower than for MDCT but still higher than those of the 3D C-arms.

Conclusions: Intraoperative imaging using 3D C-arm devices is an effective method to verify reduction results in maxillofacial surgery intraoperatively with significantly lower ED than postoperatively CBCT and MDCT imaging.

Keywords

3D-imaging, CT, conebeam CT, 3D C-arms, effective dose, organ dose

¹Department of Cranio-Maxillo-Facial-Surgery, University Hospital Ulm, Ulm, Germany

²Department of Cranio-Maxillo-Facial-Surgery, German Armed Forces Hospital Ulm, Ulm, Germany

³Institute of Anatomy, Medical Faculty, University of Leipzig, Leipzig, Germany

⁴Department of Cranio-Maxillo-Facial-Surgery, University Hospital Freiburg, Freiburg, Germany

⁵Department of Nuclear Medicine, University Hospital Ulm, Ulm, Germany

Corresponding author:

Sebastian Pietzka, Department of Cranio-Maxillo-Facial-Surgery, German Armed Forces Hospital Ulm, Germany Oberer Eselsberg 40, Ulm 89081, Germany.

Email: dr.pietzka@gmx.net

Introduction

A milestone in the history of radiography was the development of mobile X-ray units with image intensifiers. Their implementation in the 1960s allowed intraoperative two-dimensional visualisation and thus the direct examination of surgical treatments.¹⁻³ This type of intraoperative reduction control and determination of the position of osteosynthesis material after fracture treatment initially established itself as the standard for orthopaedics and trauma surgery.⁴

With the introduction of the multidetector computed tomogram (MDCT), a new gold standard for postoperative control was created for complex fractures of the joints as well as for spinal interventions. However, the transfer to the operating theatre and the establishment of regular intraoperative three-dimensional imaging only succeeded with the introduction of the 3D C-arm. The benefit of this intraoperative imaging and the associated possibility of immediate correction and consequent avoidance of revision surgery have been adequately demonstrated.³⁻⁵

Correspondingly, it was shown for oral and maxillofacial surgery that in the region of anatomically complex structures such as the facial skull and here in particular the orbit, two-dimensional intraoperative images are not sufficient for the reliable assessment of fracture restorations due to possible superimposition effects.⁶⁻⁹ Therefore, postoperative 3D imaging using MDCT or dental CBCT has been regularly recommended to evaluate the surgical outcome in oral and maxillofacial surgery after midface reconstructions.¹⁰ This was regularly done on the 1st or 2nd postoperative day. If the postoperative CT then showed incorrect positioning, a new operation often had to be planned.⁸

With the introduction of intraoperative 3D C-arms, it was possible to immediately provide surgeons with detailed intraoperative visualisation.

It has been shown that intraoperative 3D C-arm imaging leads to a reduction in morbidity in the surgical treatment of facial fractures. Furthermore, it could be shown that these intraoperative 3D images can replace postoperative imaging by MDCT or CBCT in a large number of cases.^{11,12}

In particular, the 3D C-arms of the newer generation show a high-resolution bony representation with good possibilities for multiplanar as well as three-dimensional reconstruction.¹³

To this day, however, there are no studies in the literature that compare the radiation dose of an intraoperative 3D C-arm with conventional MDCT or dental CBCT of the facial skull.

The aim of the study was therefore to compare the OD and the effective radiation dose between MDCT, dental CBCT and intraoperative 3D C-arms after typical scans of midfacial region.

Material and Method

This experimental study was submitted to the ethics committee of the University of Ulm. As no studies were carried out on humans, it was decided that no special vote was required.

Thermoluminescence dosimeters (TLD) can be used to determine the energy absorbed during an X-ray process. These TLDs store the emitted energy of the incoming radiation and, after subsequent heating during evaluation, release it again in the form of light. The generated light intensity can then be measured with the help of a photomultiplier in an electronic analyser.¹⁴

To determine the specific doses to organs and tissues, these TLDs were placed in an Alderson-Rando phantom head and the absorbed radiation of four mobile 3D C-arms, two CBCTs and one MDCT was determined for a typical 3D X-ray scan of the facial skull.

The Alderson-Rando phantom head used a real human skull embedded in rubber mass with 9 axial planes. (Figure 1). These contain 24 defined receptor points for the TLDs in the area of the sensitive organs and tissues. Through this defined positioning, the absorbed radiation can be reproducibly determined at the anatomically corresponding localisation¹⁵⁻¹⁷ (Figure 1) and the individual TLDs of the corresponding levels can be assigned to the individual organs or tissues accordingly (Table 1).

The phantom head was equipped with 24 new TLDs in the defined positions before each examination. Subsequently, the phantom skull was positioned in the corresponding 3D X-ray devices analogous to a real X-ray examination either in a lying position or sitting on a tripod (Figure 2).

Following this, the phantom head was scanned with the corresponding defined device settings. In order to avoid the risk of accidental errors, this procedure was repeated ten times in succession with the same TLDs and the results were then divided by ten again in the evaluation in order to be able to indicate the dose of a single X-ray examination of the facial skull.

After each scan series, the TLD's were analysed and the phantom re-equipped to examine the next 3D X-ray machine.

The Field of View (FoV) used should correspond to a typical facial skull image from the frontal sinus up including the mandible.

Accordingly, in computed tomography, the FoV was set according to the topogram. In the other 3D X-ray devices, the FoV that most closely corresponds to the facial skull image was selected based on the different device characteristics (Table 2).

In the group of the four mobile 3D C-arms, the Siemens® Siremobil Iso-C-3D with integrated image intensifier



Figure 1. Image of the Alderson-Rando phantom head, location of the TLDs in the nine different axial planes.

Table 1. Assignment of the TLD's to the Corresponding Organs and the Corresponding Axial Plane of the Alderson-Rando Phantom Head.

TLD	Tissue/Organ	Axial Plane
1	Calotte anterior	2
2	Calotte left	2
3	Calvaria posterior	2
4	Midbrain	2
5	Pituitary gland	3
6	Orbit left	4
7	Orbit right	4
8	Eye lens left	3
9	Eye lens right	3
10	Parotid gland left	5
11	Parotid gland right	5
12	Cheek right	5
13	Ramus left	6
14	Ramus right	6
15	Cervical spine centre	6
16	Neck posterior left	7
17	Corp. mandib. anterior	7
18	Corp. mandib. left	7
19	Gl. submand. left	8
20	Gl. submand. right	8
21	Gl. sublingualis	7
22	Thyroid surface left	9
23	Thyroid midline	9
24	Oesophagus	9

(60 kV and 4.8 mA) with an FoV of $12.3 \times 12.3 \times 12.3$ cm, the Siemens® Arcadis Orbic 3D with integrated image intensifier (64 kV and 2.2 mA) and an FoV of $12 \times 12 \times 12$ cm, the Ziehm® Vision Vario FD 3D with integrated flat panel detector (FPD) (63 kV and 16.2 mA) and an FoV of $12.8 \times 12.8 \times 12.8$ cm, and the Siemens® Cios Spin with integrated CMOS flat panel detector (FPD) (110 kV and .14 mAs) and an FoV of $16 \times 16 \times 16$ cm were examined and compared.

In the dental CBCT group, the KaVo® 3D eXam with flat panel detector (120 kV and 5 mA) and a FoV of $\varnothing 16 \times 13$ cm and the Sirona® Galileos Comfort with image intensifier (98 kV and 6 mA) and a FoV of $\varnothing 15.4$ cm were considered.

For the CT examination, the Siemens® Somatom Force 384 was used with 120 kV and 45 mAs in the default setting and with 100 kV and 25 mAs in a dose-reduced scan programme adapted for bone imaging in maxillofacial surgery with individually defined FoV according to the topogram.

In addition to the 3D scan performed, a pre-scan was performed for the 3D C-arms and the CT to create the topogram, or to position the phantom skull properly. These radiation doses should also be registered.

For these pre-scans, the phantom skull was therefore again equipped with 24 new TLDs and then the overview scan was performed in the sense of the required pre-scan. In order to obtain more reliable results despite the low doses of the pre-scans, this pre-scan was carried out 50 times with the

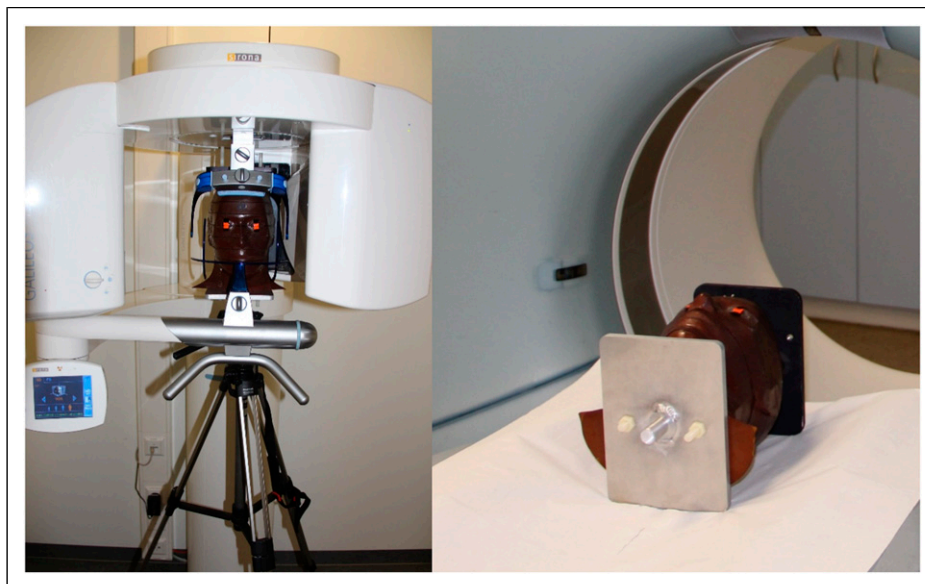


Figure 2. Alderson-Rando phantom head in the sitting position on the tripod in the CBCT Sirona®Galileos comfort and in the lying position in the Siemens®Somatom force 384.

Table 2. Field of View of the 3D C-Arm Devices and the Dental CBCTs Used During the Examination.

	Siemens®Siremobil Iso-C-3D	Siemens®Arcadis Orbic 3D	Siemens®Cios Spin	Ziehm®Vision Vario FD 3D
3D C-Arm	12.3 × 12.3 × 12.3 cm	12 × 12 × 12 cm	16 × 16 × 16 cm	12.8 × 12.8 × 12.8 cm
CBCT	KaVo® 3D eXam Ø 16 × 13 cm		Sirona®Galileos comfort Ø 15.4 cm	

same TLDs and the result was then divided by 50 in the evaluation.

Following each scan series of the individual X-ray units in the experiment, the exposed (TLD) were read out by the Karlsruhe Institute of Technology (KIT) using a TLD reader (Pitmann®, Toledo 654) and the respective absorbed doses (D) of the 24 TLDs were determined for the individual regions.

For the 3D X-ray devices where a pre-scan was necessary, the values for the pre-scan and main scan were then added together and considered together.

In addition, two control measurements were performed for each 3D X-ray device with a reduced set of only 8 TLDs. This aimed to identify device-independent measurement errors. The data of the two control measurements were then compared with those of the primary measurements and checked for possible outliers.

Subsequently, the organ equivalent dose (H_T) was determined according to the radiation weighting factor (W_r) = 1 for X-rays.

However, since only the phantom skull and not a whole phantom body was irradiated, the corresponding

Table 3. Tissue Weighting Factors for Determining the Effective Dose Recommendations of the International Commission on Radiological Protection (ICRP) Established in the Year 2007 (ICRP 103).

Organ W_T	ICRP 103
Bone marrow (red), colon, lung, stomach	.12
Chest	.12
Gonads	.08
Bladder, oesophagus, liver, thyroid	.04
Bone surface, skin	.01
Brain	.01
Salivary glands	.01
Remainder	.12

percentages determined by Ludlow and Ivanovic¹⁵ 2008 had to be used to calculate the effective dose.

Because individual tissues and organs each show different sensitivities to exposed ionising radiation, the 2007 tissue weighting factors (W_T) established by the International Commission on Radiological Protection (ICRP)

were used to calculate the effective dose in accordance with IRCP 103 (Table 3).¹⁸

The organ doses (H_T) already determined were multiplied by the respective tissue weighting factors (W_T) and then added up. In this way, the effective dose (E) could be determined via the formula

$$E = \sum_T w_T \cdot H_T$$

for all seven X-ray devices.

Results

There were substantial differences in the OD determined between the individual devices, the individual device groups, as well as a further clear variation in the individual OD of the different tissues (Table 4).

The lowest OD was measured for ‘Oesophagus’ in the Siemens® Arcadis Orbic 3D with 2 µSv. The highest, on the other hand, was in the ‘Salivary glands’ with the Siemens® Somatom Force in the basic setting with 9318.7 µSv. Accordingly, there was a large variation here.

In general, the OD determined for the 3D C-arms used were significantly lower than for all other 3D X-ray devices. But even within this group, the values varied greatly (Figure 3). The Siemens® Arcadis Orbic 3D device clearly showed the lowest values in all OD and in comparison to all other 7 devices.

The 3D C-arm Siemens® Cios Spin basically showed the second lowest values, but was in the OD of ‘Bone marrow’ (84.9 vs 77.5 µSv) and ‘Brain’ (1359.2 vs 749.5) partly even higher than the CBCT Sirona® Galileos Comfort.

The Siemens® Siremobil Iso-C-3D and the Ziehm® Vision Vario FD 3D had higher values in all OD than the other two 3D C-arms Siemens® Arcadis Orbic 3D and Siemens® Cios Spin. These two devices showed particularly high values in “Bone surface”, “Brain”, “Salivary glands”, “Upper airway” and “Oral mucosa” in the group of mobile devices (Figure 3). Particularly striking was the high ODdose to “Brain” from the Ziehm® Vision Vario FD 3D of 4003.9 µSv.

This value was higher than the OD to ‘Brain’ for all CBCTs (2272 and 749 µSv) as well as the value for ‘Brain’ of the MDCT in the reduced CMF settings (2863 µSv). Only the MDCT in the basic setting had a higher OD for ‘Brain’ with 9175.8 µSv.

In the group of stationary machines, the MDCT in the basic setting also showed by far the highest values for all OD (Figure 4).

Only by adapting the scan protocol for hard tissue in the CMF-region an OD corresponding to the CBCT could be partially achieved. However, this was still significantly

Table 4. Determined Organ Doses (H_T) for the Seven Individual 3D X-Ray Units (µSv).

	Siemens® Siremobil ISO-C-3D	Siemens® Arcadis Orbic 3D	Ziehm® Vision Vario FD 3D	Siemens® Cios Spin	KaVo® 3D eXam	Sirona® Galileos	Siemens® Somatom Force Regular	Siemens® Somatom Force CMF
Bone marrow	134.4	13.5	195.1	84.9	75.3	77.5	479.6	137.4
Oesophagus	15.6	2	21.4	17	72.5	114.5	763.8	217.1
Thyroid	120.8	17.2	225.2	106.7	637.5	994.5	9432.7	3597.4
Bone surface	589.6	58.3	807.7	174.5	150.3	225.1	962.9	278.7
Brain	1666.6	276.7	4003.9	1359.2	2272	749.5	9175.8	2863.7
Salivary glands	1606	182.6	1965.7	906.7	4003.3	4432	9318.7	2863.1
Skin	296.4	8.6	101.3	27.1	217.1	191.4	431.5	143.2
Upper airway	1822.2	186.5	1505.5	926.5	3342.1	3518.6	9243.7	2797.1
Lymphnodes	65.7	8.2	68.6	43	157.8	186.5	464.3	140.1
Muscle tissue	65.7	8.2	68.6	43	157.8	186.5	464.3	140.1
Oral mucosa	1513.5	179.3	1401.7	868.2	3906.2	4262.4	9401	2779.6

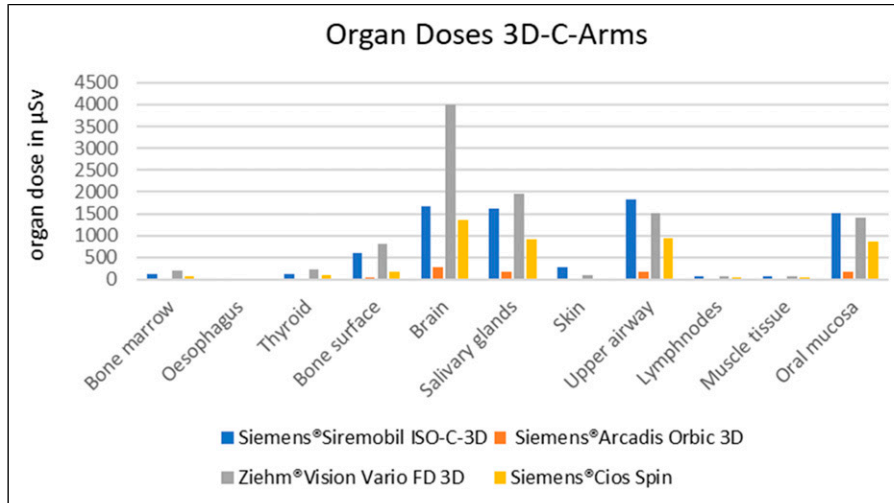


Figure 3. Graphical presentation of the organ doses determined for the 3D C-arms used.

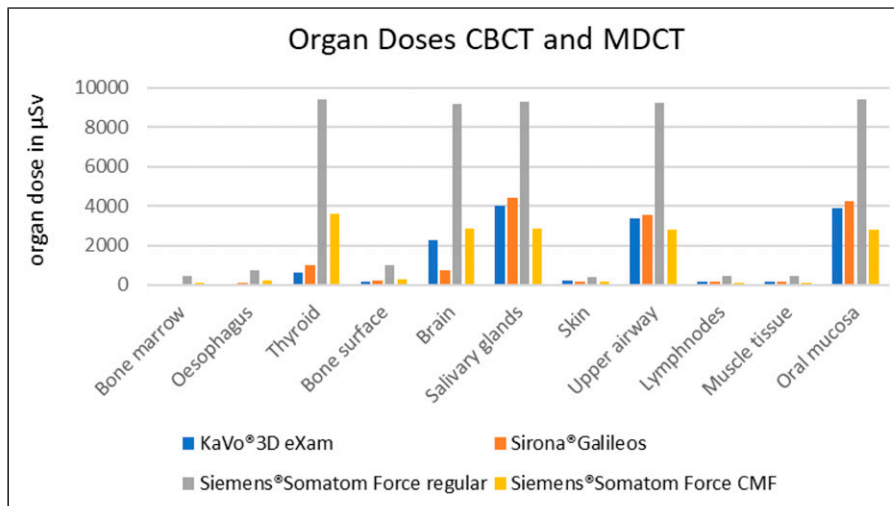


Figure 4. Graphical presentation of the organ doses determined for the CBCTs and the MDCT used.

higher in the areas of ‘Thyroid’, ‘Bone marrow’, ‘Oesophagus’ and ‘Brain’.

Only in the areas of ‘Oral mucosa’, ‘Upper airway’ and ‘Salivary glands’ a significant reduction compared to the CBCTs could be demonstrated (Figure 4).

The calculation of the ED showed similar results. The ED for the corresponding craniofacial imaging of the 7 different devices also differed significantly here. By far the lowest ED were found for the 3D C-arms (Figure 5).

The Siemens®Arcadis Orbic 3D was outstanding with a very low ED of 11.18 µSv followed by the Siemens®Cios Spin with 57.18 µSv.

These two 3D C-arms of the newer generation showed the highest image quality and detail when viewing the images clinically. In addition, the Siemens®Cios Spin also had the largest FoV of the mobile units at 16 × 16 × 16 cm.

The two other 3D C-arms of the older generation showed higher ED of 95.18 µSv for the Siemens®Siremobil Iso-C-3D and 129.9 µSv for the Ziehm®Vision Vario FD 3D. Nevertheless, these values were still below the ED of the two CBCTs KaVo®3D eXam with 173.68 µSv and Sirona®Galileos Comfort with 184.91 µSv.

The ED of the MDCT Siemens®Somatom Force 384 in the standard setting was 844.97 µSv and therefore many times higher than that of the 3D C-arms as well as the CBCTs.

The effective doses could only be reduced to values of 284.52 µSv by adjusting the scan protocol when the focus was reduced to bone imaging in the CMF. However, the ED was still above the values of the two CBCTs and clearly above the values of the 4 mobile 3D C-arms.

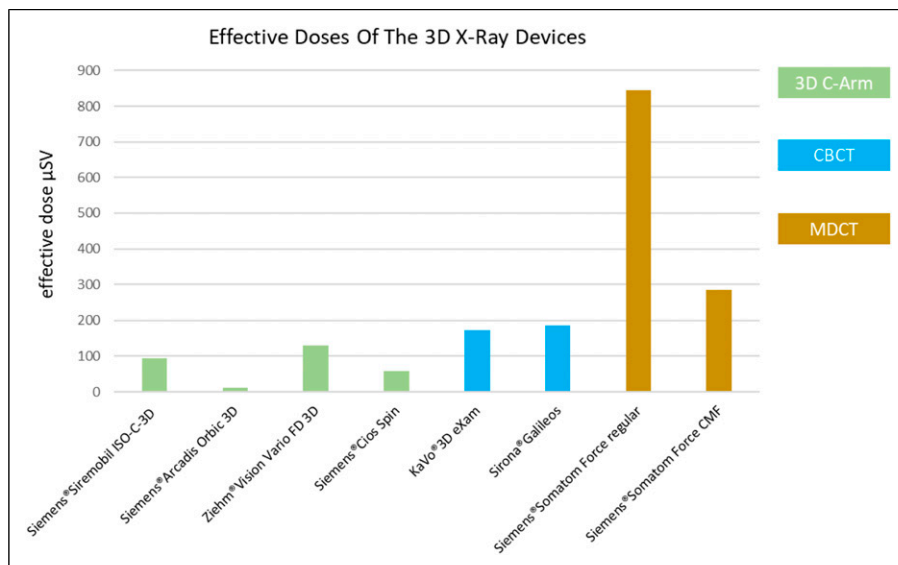


Figure 5. Graphical presentation of the effective doses of the seven different 3D X-ray devices.

The two additional control measurements with a reduced number of TLDs (8) did not show any deviations of higher values compared to the original examination. In particular, there were no deviations in which dimensions had shifted or deviations that made the examination results of individual units appear to be accidental or erroneous.

Discussion

Postoperative 3D images after complex facial skull fractures are often indicated to assess the reduction result and the position of the osteosynthesis material. In the sense of the ALARA principle, a device selection should be made in which the dose is kept as low as possible, but anatomical structures can be sufficiently depicted and assessed. However, the indication regarding usability and practicability under operating conditions also have an impact here.

The authors had not anticipated that the OD and ED would be so much lower when using the 3D C-arms compared to CBCTs or MDCT.

Therefore, the results had to be examined critically.

To determine the OD and the ED in this study, a previously established and verified method using the Alderson-Rando phantom skull was applied. There were no adaptations to the established protocol or deviations in the evaluation of the TLDs in this study. All TLDs were evaluated independently of KIT.

The positioning of the phantom skull was carried out in accordance with the settings of a real examination on humans, either in a lying or sitting position, depending on the different devices.

However, the different positioning and alignment of the phantom head due to the equipment with a possible shift of

the isocentre and the resulting change in radiation intensity on the respective organs are possible causes for the different organ exposures. However, this can also occur during a real examination and could not be consciously influenced by the authors.

Furthermore, the same phantom skull was used for the evaluation of all devices, so that possible errors due to anatomical differences could be excluded.

Therefore, the different device parameters such as tube voltage (kV), tube current (mA) and exposure time have the predominant influence on organ doses. High kV and mA settings as well as longer exposure times inevitably lead to a higher applied dose. This could also be demonstrated by the reduction of organ doses when adjusting the values in MDCT with a CMF scan protocol.

The values for the ED determined according to ICRP 103 also show clear deviations between the individual devices. For example, the data evaluation shows that the highest radiation exposure for the computer tomograph, the Siemens®Somatom Force 384, was both in the basic device setting with 845 µSv and when using the adapted scan protocol for the facial skull with 284.5 µSv.

The results of the effective doses for the mobile 3D C-arms used in this study as well as for the two DVT devices are clearly below the values of the MDCT.

However, it was also shown that the values for the two CBCTs used, 173.7 and 184.9 µSv, were higher than those of the four 3D C-arms 11.2–129.9 µSv.

The particularly low ED of the Siemens®Arcadis Orbic 3D compared to its successor Siemens®Cios Spin was surprising. This can best be explained by the significantly increased FoV of the Siemens®Cios Spin and a further improvement in the recording quality compared to its

predecessor. Furthermore, the highest quality setting was selected for the examination of the Siemens®Cios Spin. In clinical use of the device for intraoperative control, however, the lower quality setting is often used. The images generated in this way are still of good quality with a corresponding reduction in the radiation dose.

The usability of the new generation of 3D C-arms has improved significantly compared to their predecessors. The devices can be positioned quickly and safely without a pre-scan and scan time has also been reduced compared to the previous generation. In addition, these devices can now also be operated partially radiation-free for the user via a remote control from the control area. The image quality has improved significantly compared to its predecessors and the bone representation is only slightly below the quality of a CBCT or CT. However, this lower quality must also be taken into account with the lower radiation exposure.

From the authors' point of view, only significant advantages of intraoperative imaging with 3D C-arms with additional reduction of the effective dose compared to CBCT or MDCT are thus shown.

Conclusion

Intraoperative imaging using a 3D C-arm is an effective method for verifying reduction results and the position of the osteosynthesis material in complex procedures in maxillofacial surgery.

By employing an intraoperative 3D C-arm scan, the effective radiation dose can be significantly reduced, especially compared to a regular postoperative CT scan. However, the applied ED dose is still dependent on the device used. When using a device of the latest generation, such as the Siemens®Arcadis Orbic 3D, the effective dose can be significantly reduced even compared to a common postoperative dental CBCT. This is especially important to the cumulative radiation exposure of patients over the years of their lives.

Acknowledgements

The publication contains excerpts from the doctoral thesis of Anne Grieser.

Declaration of Conflicting Interests

The author(s) declared no potential conflicts of interest with respect to the research, authorship, and/or publication of this article.

Funding

The author(s) disclosed receipt of the following financial support for the research, authorship, and/or publication of this article: Open Access funding enabled and organized by Projekt DEAL.

Ethical Statement

Ethical Approval

Dear Ladies and Gentleman, this experimental study was submitted to the ethics committee of the University of Ulm. As no studies were carried out on humans, it was decided that no special vote was required. Address: Ethikkommission der Universität Ulm Barbara Mez-Starck Haus Oberberghof 7 89081 Ulm.

ORCID iDs

Sebastian Pietzka  <https://orcid.org/0000-0002-9559-2306>

Michael Grunert  <https://orcid.org/0000-0001-8056-7290>

References

- Gebhard F, Riepl C, Richter P et al. [The hybrid operating room. Home of high-end intraoperative imaging]. *Unfallchirurg*. 2012;115:107-120. doi:10.1007/s00113-011-2118-3
- Wich M, Spranger N, Ekkernkamp A. [Intraoperative imaging with the ISO C(3D)]. *Chirurg*. 2004;75:982-987. doi:10.1007/s00104-004-0953-2
- Stengel D, Wich M, Ekkernkamp A, Spranger N. [Intraoperative 3D imaging: Diagnostic accuracy and therapeutic benefits]. *Unfallchirurg*. 2016;119:835-842. doi:10.1007/s00113-016-0245-6
- Schnetzer M, Fuchs J, Vetter SY et al. Intraoperative 3D imaging in the treatment of elbow fractures—a retrospective analysis of indications, intraoperative revision rates, and implications in 36 cases. *BMC Med Imag*. 2016;16:24. doi:10.1186/s12880-016-0126-z
- von Recum J, Wendl K, Vock B, Grütznert PA, Franke J. [Intraoperative 3D C-arm imaging. State of the art]. *Unfallchirurg*. 2012;115:196-201. doi:10.1007/s00113-011-2119-2
- Hanken H, Lohse C, Assaf AT, Heiland M. Intraoperative Bildgebung in der Mund-Kiefer- und Gesichtschirurgie. *OP-Journal*. 2014;29:130-135. doi:10.1055/s-0033-1350665
- Füßinger MA, Duttenehofer F, Bittermann G, Schmelzeisen R. [Intraoperative quality management modalities in head and neck surgery]. *HNO*. 2016;64:650-657. doi:10.1007/s00106-016-0203-1
- Stanley RB. Use of intraoperative computed tomography during repair of orbitozygomatic fractures. *Arch Facial Plast Surg*. 1999;1:19-24. doi:10.1001/archfaci.1.1.19
- Manson PN. Computed tomography use and repair of orbitozygomatic fractures. *Arch Facial Plast Surg*. 1999;1:25-26. doi:10.1001/archfaci.1.1.25
- Fiebich M, Weber D. [Digital volume tomography: Dedicated scanner and cone beam CT with C-arm systems]. *Radiologe*. 2018;58:194-201. doi:10.1007/s00117-018-0360-1

11. Wilde F, Schramm A. [Computer-aided reconstruction of the facial skeleton: Planning and implementation in clinical routine]. *HNO*. 2016;64:641-649. doi:[10.1007/s00106-016-0220-0](https://doi.org/10.1007/s00106-016-0220-0)
12. Wilde F, Lorenz K, Ebner A-K, Krauss O, Mascha F, Schramm A. Intraoperative imaging with a 3D C-arm system after zygomatico-orbital complex fracture reduction. *J Oral Maxillofac Surg*. 2013;71:894-910. doi:[10.1016/j.joms.2012.10.031](https://doi.org/10.1016/j.joms.2012.10.031)
13. Kraus M, Fischer E, Gebhard F, Richter PH. Image quality and effective dose of a robotic flat panel 3D C-arm vs computed tomography. *Int J Med Robot*. 2016;12:743-750. doi:[10.1002/rcs.1718](https://doi.org/10.1002/rcs.1718)
14. Krieger H. *Strahlungsmessung und Dosimetrie, 2., überarb. u. erw. Aufl. 2013*. Wiesbaden: Springer Fachmedien Wiesbaden Imprint Springer Spektrum; 2013.
15. Ludlow JB, Ivanovic M. Comparative dosimetry of dental CBCT devices and 64-slice CT for oral and maxillofacial radiology. *Oral Surg Oral Med Oral Pathol Oral Radiol Endod*. 2008;106:106-114. doi:[10.1016/j.tripleo.2008.03.018](https://doi.org/10.1016/j.tripleo.2008.03.018)
16. Ludlow JB, Davies-Ludlow LE, Brooks SL, Howerton WB. Dosimetry of 3 CBCT devices for oral and maxillofacial radiology: CB Mercuray, NewTom 3G and i-CAT. *Dentomaxillofacial Radiol*. 2006;35:219-226. doi:[10.1259/dmfr/14340323](https://doi.org/10.1259/dmfr/14340323)
17. Schilling R, Geibel M-A. Assessment of the effective doses from two dental cone beam CT devices. *Dentomaxillofacial Radiol*. 2013;42:20120273. doi:[10.1259/dmfr.20120273](https://doi.org/10.1259/dmfr.20120273)
18. (2007) The 2007 Recommendations of the International Commission on Radiological Protection. ICRP publication 103. *Ann ICRP*. 2007;37:1-332. doi:[10.1016/j.icrp.2007.10.003](https://doi.org/10.1016/j.icrp.2007.10.003)